

# Are Out-of-Distribution Detection Methods Reliable?

Vahid Reza Khazaie\*

Anthony Wong<sup>†</sup>Mohammad Sabokrou<sup>‡</sup>

## Abstract

*This paper establishes a novel evaluation framework for assessing the performance of out-of-distribution (OOD) detection in realistic settings. Our goal is to expose the shortcomings of existing OOD detection benchmarks and encourage a necessary research direction shift toward satisfying the requirements of real-world applications. We expand OOD detection research by introducing new OOD test datasets CIFAR-10-R, CIFAR-100-R, and MVTec-R, which allow researchers to benchmark OOD detection performance under realistic distribution shifts. We also introduce a generalizability score to measure a method’s ability to generalize from standard OOD detection test datasets to a realistic setting. Contrary to existing OOD detection research, we demonstrate that further performance improvements on standard benchmark datasets do not increase the usability of such models in the real world. State-of-the-art (SOTA) methods tested on our realistic distributionally-shifted datasets drop in performance for up to 45%. This setting is critical for evaluating the reliability of OOD models before they are deployed in real-world environments.*

## 1. Introduction

Out-of-distribution (OOD) detection aims to identify samples that deviate from the norm. When the distribution of normal data contains multiple semantic concepts, detecting OOD samples by learning intrinsic concepts of in-distribution (ID) samples becomes a very challenging and cumbersome task. The inability to detect such samples compromises the reliability of machine learning methods. Therefore, OOD detection is an extremely critical task for the development of trustworthy and reliable machine learning systems [20, 24].

In recent years, a vast amount of research has been conducted on this topic. Methods such as CSI [22], ODIN [14], and PANDA [16] have saturated performance on standard OOD benchmarks, indicating that this field has reached its peak. However, this brings up the question of whether cur-

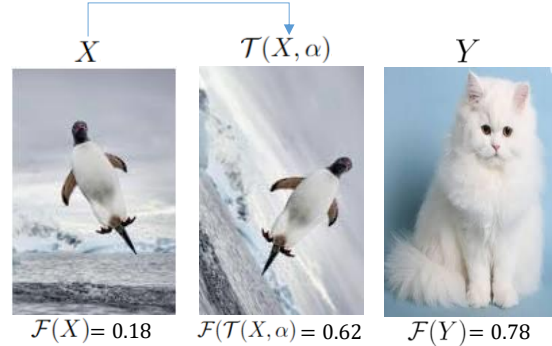


Figure 1. Example of an out-of-distribution (OOD) detector  $\mathcal{F}$  trained to detect Penguins.  $\mathcal{F}$  is a state-of-the-art OOD detector which recognizes  $X$  as an inlier and  $Y$  as an OOD sample with high confidence but fails to recognize  $\mathcal{T}(X, \alpha)$  which is the semantic-preserving transformation of an inlier. As shown in the figure,  $\mathcal{F}(X) \ll \mathcal{F}(\mathcal{T}(X, \alpha))$  and  $\mathcal{T}(X, \alpha)$  will be labeled as an OOD sample. As a result, this compromises the reliability and safety of OOD detection methods.

rent state-of-the-art (SOTA) methods are effective in real-world settings. We believe that it is time to take a step back and analyze the status quo of this research area.

We observe that the requirements of real-world OOD detection methods are not reflected by current testing protocols. Current SOTA methods have the inductive bias that during test time, normal samples have an identical distribution to the training set while anomalies are distributed further. However, real-world test samples often contain various levels of distribution shift while maintaining semantic consistency. As an example, we can think of a factory that expects that a normal screw and a screw transformed by a semantic-preserving geometric function like  $\mathcal{T}$  will produce the same result. Examples of geometric transformations of an image can be seen in Fig. 4. However,  $\mathcal{T}$  can cause shifts in distribution which compromises the performance of most SOTA OOD detection methods (See Fig. 1).

This unreliability of OOD methods is due to the above-mentioned inductive bias. In fact, the current SOTA are vulnerable against  $\mathcal{T}$ . Looking at current testing protocols, such distribution shifts are not taken into account in current benchmark datasets like CIFAR-10 and CIFAR-100, which have low diversity of in-distribution (ID) samples and se-

\*Vector Institute, Toronto, Canada

<sup>†</sup>Western University, London, Canada

<sup>‡</sup>Institute for Research in Fundamental Sciences (IPM), Tehran, Iran

mantically distant OOD samples. Thus, the flawed testing protocol encourages methods to have strong bias towards a low level of diversity in normal data, which is detrimental to the methods’ real-world deployability. For example, in some SOTA models such as CSI [22] the decision boundary lies extremely close to the ID samples, allowing the method to easily detect the far OOD samples. This is a consequence of using transformations of inliers as OOD samples with the contrastive learning paradigm. As a result, they ignore the variations within the inlier sets. Consequently, under realistic conditions, we believe these assumptions are insufficient for developing reliable and high-performance methods. Moreover, future research that simply improves performance on existing OOD benchmarks is not advancing the field towards more real-world applicable OOD detection methods.

At its core, changing the direction of research requires a testing protocol that represents realistic conditions and an evaluation metric to quantify how well the problem has been solved. To better reflect the conditions in the real world, we propose a new benchmark evaluation framework consisting of new OOD detection benchmark test sets and a new metric. To create our test sets, one potential method of increasing diversity in distribution shifts while maintaining semantic meaning is to combine existing datasets. However, this is limited by the fact that finding semantically matching classes across datasets is not always possible for research and in real-world applications. Thus, we must create an OOD detection benchmark that simultaneously contains sufficient intra-class distribution shift while maintaining semantic meaning. This can be achieved using common corruptions [10] and augmentations. Common corruptions are purposefully designed image perturbations that mimic frequently encountered perturbations in natural images [10]. Models are expected to be robust to images with common corruptions because such samples maintain semantic meaning. Augmentations are realistic transformations applied to data to increase its diversity without disturbing the semantic meaning of the transformed image. Our benchmark is created from existing datasets, such as CIFAR-10, CIFAR-100 and MVTec AD, by applying common corruptions and augmentations. Our evaluation metric measures the difference in performance between previous benchmarks and our proposed benchmark. If a method can generalize to all in-class distribution shifts, the difference will be zero. Our proposed evaluation framework simultaneously measures both OOD detection performance and generalization. As a result, we suggest that future OOD detection methods follow this research avenue.

The main contributions of this paper are the following:

- We propose a novel evaluation framework for out-of-distribution detection methods and demonstrate why it better represents real-world conditions.

- We introduce new out-of-distribution detection test sets and a generalizability score to quantify performance differences between the existing benchmarks versus our proposed evaluation framework.
- We show that state-of-the-art methods fail to perform well on our proposed benchmark, indicating that they cannot reliably be applied to the real world and that current benchmarks are not true indicators of performance.

## 2. Related Works

Reconstruction-based anomaly detection is a classical approach that uses the training set to learn patterns that reflect the normal data in an effective way. Based on the learned semantic features, they attempt to reconstruct a new sample at test time. The method assumes that normal data will be reconstructed well, while abnormal data cannot. Samples are classified as normal or anomalous based on thresholds applied to reconstruction error. For instance, a model for video outlier detection suggested by Cong et al. [6] included sparse representations to distinguish inliers from outliers. Using representations learned from inlier data and the reconstruction error, [17, 23] detects out-of-distribution data. Several deep learning models with encoder-decoder architecture have also used this score to detect anomalies [5, 19, 27–29]. While these methods are effective, they are limited by their poorly designed latent space. In [8], a deep autoencoder augmented by a memory module for anomaly detection was proposed by Gong et al. to encode the input into a latent space which constrains it to store a small number of key features of inliers. The main weakness of reconstruction-based methods is the problem of not learning discriminative basis function, as well as reconstructing outliers with low error in cases when they share common patterns with inliers.

In addition, adversarial training can be utilized to detect out-of-distribution data. By combining Generative Adversarial Networks (GANs) [9] with denoising autoencoders, Sabokrou et al. [18] proposed a one-class classifier for novelty detection which uses the discriminator’s score for reconstructed samples. By modifying the discriminator role to distinguish between good and bad reconstruction quality, Zaheer et al. redefined the adversarial one-class classifier training setup to improve its results [25]. In [26], a new unsupervised generative learning approach for video anomaly detection exploits the low frequency of anomalies by building cross-supervision between generators and discriminators. To force normal samples to be distributed uniformly across the latent space, Perera et al. used denoising autoencoder networks [15] in an adversarial manner. In [12], an adversarial setup is utilized to mask the input of the autoencoder intelligently and learn more robust representations.

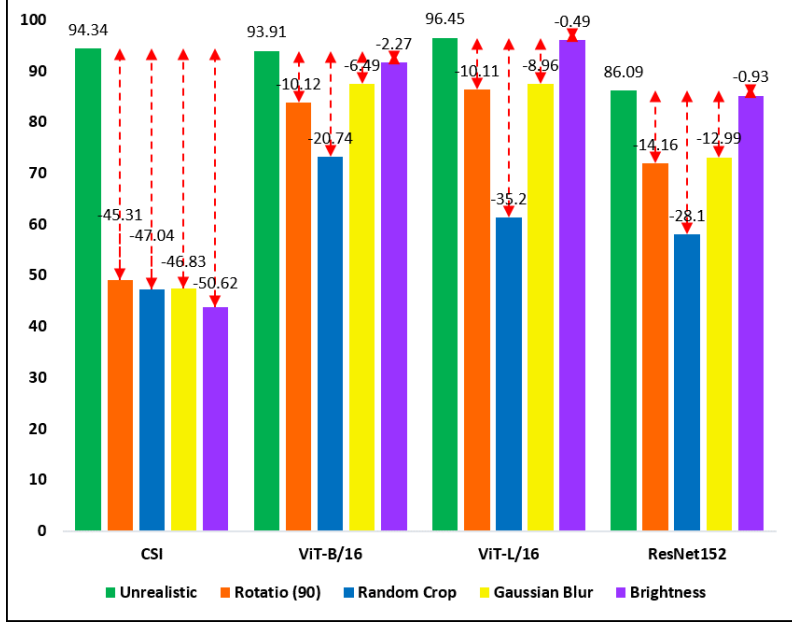


Figure 2. This figure compares the performance of multiple SOTA models. The green bars display the performance of these models on existing OOD detection benchmarks, whereas the other bars display the performance of the same method on the same dataset but also includes samples transformed by  $\mathcal{T}$ . We can observe a drastic drop in performance caused by a single  $\mathcal{T}$ . This clearly displays the consequence of inductive bias in SOTA methods as a result of existing testing protocols. Therefore, metrics reported by existing evaluation frameworks do not represent real-world performance.

A deep autoencoder with a parametric density estimator is proposed by [1] with an autoregressive procedure to learn its latent representations. In spite of showing success in some OOD detection scenarios, training instability is a limitation of this category of methods.

There are also methods that use contrastive and self-supervised techniques. For self-supervised anomaly detection, Rot [11] uses an auxiliary task of rotation prediction. By using rotation-prediction methods, GOAD [3] learns a feature space in which the inter-class separation between normal data is relatively small. Methods such as CSI leverages contrastive learning paradigm to contrast against distribution-shifted augmentations of the data samples along with other samples. In SSD [21], anomalies are scored by the Mahalanobis distance based on K-means clusters. These types of methods may perform well on current benchmarks, but they have some unrealistic assumptions about out-of-distribution data when augmentations such as rotation are applied. This can compromise their reliability in cases where the semantic meaning remains consistent over distribution shifts of inlier data.

The performance of out-of-distribution detection methods can be significantly improved when pre-trained representations are leveraged. An autoencoder was suggested to map normal training data closer together with a compactness loss on pre-trained features. These techniques were applied to ImageNet pre-trained representations and later

refined through self-supervised feature adaptation. Based on pre-trained features, DN2 [2] estimates density using kNNs. Each sample is scored according to the distance from its nearest normal training image. In the case of a larger distance, there is a lower density of normal samples, so an abnormality is more likely to occur. Most of the models evaluated on our proposed testing framework in this paper use the same approach.

### 3. Realistic OOD Detection Benchmark (ROOD)

#### 3.1. Problem Definition

To begin, we define the existing OOD detection benchmark setup. Inlier training data is represented as  $X = [X_1 \dots X_n]$ . Combining the inlier test data  $X' = [X'_1 \dots X'_n]$  and OOD test data  $Y = [Y_1 \dots Y_n]$ , the test set  $S$  is formulated by their union:  $S = \{Y \cup X'\}$  where  $Y \not\approx \mathcal{P}_I$  and  $X' \approx \mathcal{P}_I$ . We define  $\mathcal{P}_I$  as the distribution of inliers. In general, training OOD detection method involves optimizing the parameters  $\theta$  of a function such as  $\mathcal{F}_\theta(Z)$  such that it outputs an OOD detection score of a sample  $Z$ . Similarly, conventional OOD methods are optimized on  $X$  and detect the OOD samples by thresholding on the output of learned  $\mathcal{F}$ . As previously mentioned, current methods are designed based on hypothesis  $\mathbf{H}$  which is defined in Equ. 1.

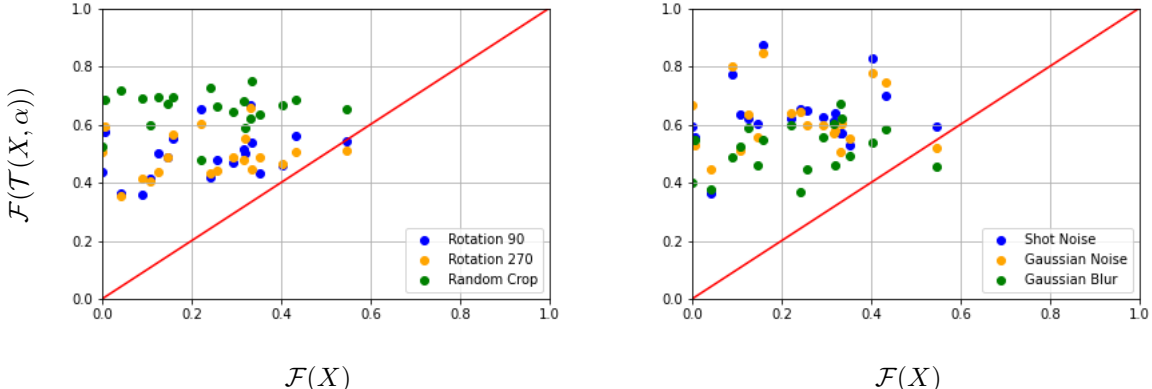


Figure 3. Each figure contains 20 data points and plots the OOD score produced by ViT-B/16 of an inlier sample  $X$  against the OOD score of the same inlier sample  $X$  transformed by  $\alpha$ . Those samples used in the left figure have been transformed by 3 augmentations, while those on the right are transformed by 3 common corruptions. As demonstrated, the OOD score for most of the samples has been increased towards one after applying  $\mathcal{T}$ . This shows the current SOTA models’ low generalizability on  $\mathcal{T}$  which doesn’t change the semantic meaning of the data. An ideal model will produce the same score for an inlier sample  $X$  even after applying  $\mathcal{T}$  ( $\mathcal{F}(X) = \mathcal{F}(\mathcal{T}(X, \alpha))$ ).

$$\mathbf{H} : \forall X_i, X_j \approx \mathcal{P}_I \text{ and } \forall X_l \not\approx \mathcal{P}_I \quad (1)$$

$$\mathcal{D}(X_i, X_j) \ll \mathcal{D}(X_i, X_l)$$

Where,  $\mathcal{D}$  computes the whole difference (i.e, consider both semantic and non-semantic features) between two images. In a real-world application, it is expected that  $\mathcal{D}$  utilizes only semantic features to make decisions. Being sensitive to the non-semantic features leads to failure when the model faces ID samples altered using semantic preserving transformations.

Here, we propose a new benchmark which better represents real-world conditions and demonstrates that current SOTA methods fail in such a benchmark. An ideal and robust OOD detector should output the same OOD score i.e  $\mathcal{F}_\theta(X)$  for an inlier sample that is non-semantically changed by some transformations  $\alpha$  (e.g,  $\alpha$  can be a rotation). Ideally, the OOD score must be the same ( $(\mathcal{F}(X) - \mathcal{F}(\mathcal{T}(X, \alpha))) < \epsilon$ ) where  $\epsilon$  is a very small value close to zero. In other words, the method should be robust to transformations such as  $\mathcal{T}$ . In this paper, we show that most of the SOTA OOD methods fail in the above-mentioned setup. This means ( $(\mathcal{F}(X) - \mathcal{F}(\mathcal{T}(X, \alpha))) >> \epsilon$ ). If the difference between  $\mathcal{F}(X)$  and  $\mathcal{F}(\mathcal{T}(X, \alpha))$  is large,  $\mathcal{T}(X, \alpha)$  will very likely be labeled as OOD, which compromises the reliability of OOD detection methods in the presence of  $\alpha$ . Therefore, we introduce new realistic benchmarks and define a new score for evaluating the effectiveness of models to consider both performance and generalizability. To compare the performance of SOTA methods between our benchmarks versus current benchmarks, we define a geometric transformation function  $\mathcal{T}(S, \alpha)$  parameterized by a sample  $Z$  and transformation set  $\alpha$  where we expect  $\mathcal{F}(X)$  to

be similar to  $\mathcal{F}(\mathcal{T}(X, \alpha))$ . Elements of the geometric transformation set  $\alpha$  will guarantee semantic consistency with the input sample  $X$ . We show that many SOTA methods will have  $\mathcal{F}(X) \ll \mathcal{F}(\mathcal{T}(X, \alpha))$  by a large margin (see Fig. 3 and Fig. 2).

### 3.2. Proposed Evaluation Framework

We propose a new evaluation framework that better reflects the method’s performance in the real world. This is achieved by creating a test dataset that contains sufficient intra-class distribution shifts while maintaining semantic meaning. As such, we define the new test datasets as  $Y' = \{(Y \cup X' \cup T(X', \alpha))\}$  where  $\alpha \in C \parallel \alpha \in A \parallel \alpha \in \emptyset$ .  $C$  is the set of common corruptions, and  $A$  is the set of data augmentations. Following [10], elements in set  $C$  include gaussian noise, shot noise, impulse noise, defocus blur, glass blur, motion blur, zoom blur, snow, frost, fog, brightness, contrast, elastic, pixelate, JPEG, speckle noise, gaussian blur, spatter and saturate, all of which are frequently encountered in natural images and maintain semantic consistency with the original image. Similar to [10], we also utilize five levels of severity when applying common corruptions to the image. Set  $A$  consists of  $90^\circ$  rotation,  $270^\circ$  rotation, flip, random crop, and color jitter, all of which intuitively maintain semantic similarity with the original image. Breaking down the resulting datasets, it consists of  $Y$  and  $X'$  which is identical to the original test framework and also  $T(X', \alpha)$  which contains semantic-preserving transformations to create intra-class distribution shifts. If  $\alpha \in \emptyset$  then the test dataset is identical to the existing framework.

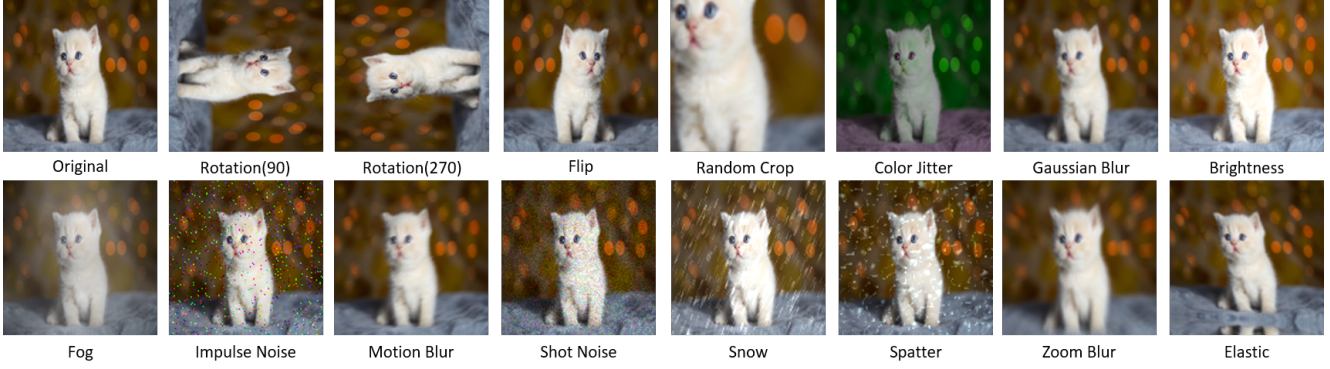


Figure 4. To better represent real-world conditions, we propose a new OOD detection test setup. To create the datasets, we propose applying semantic-preserving transformations  $\alpha$  to the inlier set  $X$ , as defined by  $\mathcal{T}(X, \alpha)$ . The examples of these transformations are mentioned in section 3.2. Provided is the results of such transformations on an image of a cat. Note that the concept of a cat is preserved in all instances.

Table 1. This table shows AUROC in % for out-of-distribution (OOD) detection on CIFAR-10 [13] dataset. GS stands for Generalizability Score (the higher, the better), and the setups **U**, **C**, and **A** are Unrealistic, Common Corruptions and Augmentations, respectively. As shown, SOTA model performance has saturated on the unrealistic setup, which is the existing OOD detection benchmark. But under transformation  $\alpha$  which consists of common corruptions and augmentations, the performance drops drastically. Notice that the highest generalizability score results from the method with the lowest AUROC under the unrealistic setting and vice versa. This indicates that high performing models sacrifice generalizability in favor of AUROC performance.

Setup	Method	Plane	Car	Bird	Cat	Deer	Dog	Frog	Horse	Ship	Truck	Mean	GS
<b>U</b>	ResNet50	82.37	79.06	68.40	58.93	84.08	56.42	82.19	71.06	84.30	87.61	75.44	N/A
	ResNet152	85.86	92.97	79.68	70.71	88.18	81.01	88.02	89.12	90.94	94.36	86.09	N/A
	ViT-B/16	95.59	96.55	90.10	88.55	94.56	88.40	95.65	97.72	96.19	95.79	93.91	N/A
	ViT-L/16	97.17	98.29	94.77	91.78	97.35	93.36	97.85	99.10	97.36	97.46	<b>96.45</b>	N/A
	CSI	89.83	99.09	93.48	86.63	93.88	93.30	95.16	98.69	97.85	95.49	94.34	N/A
<b>A</b>	ResNet50	77.34	62.48	68.33	63.38	84.44	53.54	83.35	59.73	72.18	72.84	69.76	<b>-5.68</b>
	ResNet152	72.21	69.66	60.02	55.26	69.73	60.43	77.19	58.14	72.78	73.73	66.91	-19.18
	ViT-B/16	83.41	75.85	78.29	85.90	84.67	71.55	93.82	70.29	76.51	74.60	<b>79.49</b>	-14.42
	ViT-L/16	79.18	74.14	78.63	76.06	81.12	76.97	90.60	73.36	72.67	74.73	77.75	-18.7
	CSI	49.16	66.35	9.18	1.54	52.96	55.56	1.50	91.70	73.24	88.71	48.99	-45.35
<b>C</b>	ResNet50	77.69	71.55	69.14	63.50	84.74	59.70	85.13	69.67	79.66	80.84	74.16	<b>-0.28</b>
	ResNet152	74.16	76.47	63.98	61.59	77.67	67.02	82.20	74.73	76.55	79.81	73.42	-12.67
	ViT-B/16	82.71	81.49	76.83	76.88	87.48	74.55	91.56	84.46	82.81	80.98	81.98	-11.93
	ViT-L/16	83.24	84.34	78.90	75.92	86.52	78.79	90.40	88.19	82.69	82.52	<b>83.15</b>	-13.30

### 3.3. Generalizability Score (GS)

With the definition of the new test dataset  $Y'$  we can investigate other evaluation metrics of SOTA OOD methods. As per OOD detection benchmark, we only calculate Area Under the Curve (AUROC) for each class and report the performance but in our proposed evaluation framework, we introduce a generalizability score  $GS$  which is defined as the following:

$$GS = \mathcal{F}(\mathcal{T}(Z, \alpha)) - \mathcal{F}(Z) \quad (2)$$

$GS$  is defined as the AUROC of a method tested on  $(Y \cup X')$  subtracted from the AUROC of the same method

tested on  $Y'$ .  $GS$  is designed to measure how well a method is able to generalize to intra-class distribution shifts. If the  $GS$  is negative, then the method obtains lower AUROC on  $Y'$  than  $(Y \cup X')$ . If  $GS$  is zero, then the method can be said to generalize perfectly to intra-class distribution shifts. If  $GS$  is positive, then the method performs better on intra-class distributionally shifted data than the original testing framework. Therefore, a higher  $GS$  indicates that the method being tested is more applicable to real-world applications.

Table 2. This table reports the AUROC in % for out-of-distribution (OOD) detection on CIFAR-100 [13] dataset (Super Class). We define three setups U, A, and C which represent the Unrealistic setup (existing OOD detection benchmarks), Augmentation setup, and Corruption setup. The same metrics and setups as table 1 were used for this experiment.

Setup	Method	Mean	GS
U	ResNet50	76.80	N/A
	ResNet152	85.11	N/A
	ViT-B/16	92.12	N/A
	ViT-L/16	<b>94.86</b>	N/A
A	ResNet50	74.86	<b>-1.93</b>
	ResNet152	72.69	-12.42
	ViT-B/16	<b>81.92</b>	-10.20
	ViT-L/16	79.16	-15.70
C	ResNet50	75.28	<b>-1.52</b>
	ResNet152	75.15	-9.96
	ViT-B/16	82.00	-10.12
	ViT-L/16	<b>82.14</b>	-12.72

## 4. Experimental Results

In this section, we demonstrate how current SOTA methods fail under our evaluation framework, showing that previous benchmarks are not indicative of a method’s real-world OOD detection performance. A paradigm shift is necessary because research that continues to focus on improving existing benchmarks is not guaranteed to reflect its usability.

In accordance to section 3.2, we utilize existing benchmark datasets in the creation of datasets in our evaluation framework. These include CIFAR-10 [13], CIFAR-100 [13], and MVTec AD [4]. In the following, we provide descriptions and protocols defined on each dataset.

**CIFAR-10:** Consists of 32 x 32 RGB images over 10 classes of natural objects. CIFAR-10 was previously considered to be a challenging OOD detection dataset. However, the SOTA methods’ performance saturation under the existing evaluation framework indicates that this task is becoming too simplistic.

**CIFAR-100:** consists of 32 x 32 RGB images over 100 classes of natural objects. The 100 classes can be grouped into a ‘coarse-grained’ setting of 20 super classes. We report performance using the coarse-grained setting.

**MVTec AD:** is a natural image defect detection dataset that mimics real-world industrial inspection scenarios. It contains 5354 high-resolution images over object and texture categories and over 70 types of defects such as scratches. Images sizes range from 700 x 700 to 1024 x 1024.

### 4.1. Dataset Creation

With all the previously mentioned datasets, we formulate three settings: Unrealistic ( $T(X', \alpha), \alpha \in \emptyset$ ), Common Corruptions ( $T(X', \alpha), \alpha \in C$ ), and Augmentations ( $T(X', \alpha), \alpha \in A$ ). Refer to Fig. 4 to see examples of an original image and its augmentations and common corruptions. We name our created datasets by appending R to each source dataset name for OOD detection benchmarking. As seen in Tab. 4, our evaluation framework consists of the following datasets: CIFAR-10-R which contains of the original 10000 test images, 50000 augmented images which were created by 5 different augmentations and 950000 images which were created with 19 different common corruptions with 5 level of severity (950000 = 19000  $\times$  5). CIFAR-100-R is similar to CIFAR-10-R and MVTec AD-R consists of the original test set of size 467 plus 2335 augmented images. We did not include common corruptions of inlier images in the MVTec AD dataset because it will semantically justify a defect which is not in alignment with our goal in this dataset.

### 4.2. Testing Methodology

Our testing protocol follows the one-class classification framework. During each training session, one class will be selected to be the set of inliers. When testing OOD detection using our framework, the same training class will be considered inliers in the test set, as well all semantic preserving augmentations and common corruptions will also be considered inliers. The rest of the test set which are the samples from other classes will be considered outliers. SOTA methods will be trained in this manner and results will be reported by the AUROC over the outputted OOD score.

The SOTA methods used in this paper are distance-based methods based on pre-trained feature [2], and a contrastive method from CSI [22]. For distance-based methods, we obtain representations of an anomaly detection dataset using multiple models with different architectures pre-trained on ImageNet [7]. An abnormality is more likely to occur if the distance between each sample and its nearest normal training image is larger. We also report the OOD detection results of CSI. We chose to leverage pre-trained features because they are trained on large datasets and have richer semantic features. In contrast, other OOD detection methods which require training on inlier data cannot capture such features. We hypothesize that pre-trained-based methods will perform well on our evaluation framework. On the other hand, we analyze CSI which makes the incorrect assumption of using image transformations to simulate outliers, as mentioned in section 4.3. We hypothesize that this category of methods will perform poorly on our evaluation framework.

Table 3. AUROC in % for out-of-distribution (OOD) detection on MVTec AD [4] dataset under unrealistic (U) setup and our proposed setup with contains only Augmentations (A) in this case.

Setup	Method	Bottle	Cable	Capsule	Carpet	Grid	Hazelnut	Leather	Metal Nut	Pill	Screw	Tile	Toothbrush	Transistor	Wood	Zipper	Mean	GS
U	ResNet50	97.53	78.24	82.68	78.97	59.89	92.25	96.33	76.58	69.61	70.71	94.62	89.44	85.54	95.61	92.43	84.03	N/A
	ResNet152	96.82	78.86	89.86	89.52	61.48	89.39	99.42	82.16	65.30	71.10	99.27	85.83	85.99	97.89	95.37	85.88	N/A
	ViT-B/16	99.68	88.99	79.61	85.07	81.78	93.35	100	91.69	74.93	83.91	99.13	94.16	86.91	82.28	95.24	89.11	N/A
	ViT-L/16	99.76	89.91	74.07	88.40	76.60	90.14	94.08	87.58	85.84	70.81	98.84	90.00	80.33	83.07	91.70	86.74	N/A
	ViT-L/14 (CLIP)	99.04	77.97	88.99	98.91	87.21	94.42	99.96	97.21	90.69	84.44	99.20	93.88	78.58	99.73	94.40	<b>92.31</b>	N/A
A	ResNet50	83.44	59.71	26.19	79.02	43.54	79.14	82.96	64.25	32.11	44.58	93.62	42.83	37.70	53.28	49.43	58.12	-25.91
	ResNet152	8111	59.69	32.14	76.86	42.07	78.93	78.72	68.93	33.58	46.56	97.97	43.05	40.09	54.42	55.56	59.31	-26.57
	ViT-B/16	85.22	68.31	34.83	80.20	70.67	76.91	91.55	83.92	36.71	47.33	98.64	47.88	41.68	43.70	53.77	64.09	<b>-25.02</b>
	ViT-L/16	86.52	72.79	30.05	82.56	65.79	73.29	81.63	75.70	39.30	42.21	97.41	42.77	41.36	43.03	45.14	61.30	-25.44
	ViT-L/14 (CLIP)	81.65	58.12	28.47	93.08	80.90	74.82	91.66	86.74	24.30	41.58	95.82	56.38	43.91	88.22	45.95	<b>66.11</b>	-26.20

Table 4. Our created dataset statistics.  $\|A\|$  and  $\|C\|$  indicate the number of augmentation and number of common corruption samples.

Dataset	$\ A\ $	$\ C\ $
CIFAR-10-R [13]	50000	950000
CIFAR-100-R [13]	50000	950000
MVTec AD-R [4]	2335	-

### 4.3. Evaluation and Discussion

Tab. 1, Tab. 2, and Tab. 3 show the results of SOTA methods under existing benchmark datasets as well as our created datasets. Provided in the table are the class-wise AUROC scores, the average AUROC scores over all classes, and the Generalizability Score  $GS$  to indicate the method’s applicability to the real world. Comparing the results on our datasets versus the existing benchmark datasets, we can clearly quantify the drop in performance of SOTA methods under common corruptions and augmentations. Further, we can see which methods are more susceptible to common corruptions or augmentations. A key example is the contrastive learning OOD detection method such as CSI, where rotated inlier images are simulated as anomalies during training. This will cause the model to learn closest decision boundary to the inlier training distribution. As a result, this model will fail to generalize to semantic-preserving distribution shifts. We argue that this assumption is an inductive bias that limits CSI’s applicability to the real world. Rotation is known to cause distribution shift but retain semantic knowledge. CSI’s weakness to augmentations such as rotation is clearly shown in its  $GS$  value of -45.35 when tested on CIFAR-10-R where  $(T(X', \alpha), \alpha \in A)$ , which is significantly lower than other methods that did not have such strong inductive bias against the rotation augmentation. Another observation is that while ResNet50 has among the lowest-performing AUROCs in unrealistic setups, it consistently holds the greatest  $GS$  score. We hypothesize that having the lowest number of parameters of all models limits its ability to tightly overfit to the the inlier distribution. Simultaneously, the bias-variance tradeoff tells us that a model that overfits less will have an increased capability for

generalizing to new data. This now begs the question, if CSI has among the highest AUROC in the unrealistic setting but the lowest  $GS$  score, is it a truly better-performing model than the ResNet50 with the lowest AUROC and highest  $GS$  score? In a real-world setting, it may be that ResNet50 is the higher-performing model.

Fig. 2 provides a more fine-grained study of the effects that some common corruption and augmentations have on SOTA method’s AUROC performance. The figure clearly shows the specific semantic-preserving transformations that cause distribution shifts such that SOTA methods fail, and by how much the performance will drop. The existence of such transformations is proof that SOTA methods fail to learn robust features from the inlier training data. Studying such distribution shifts is critical to choosing which real-world applications SOTA OOD detection methods can be applied to. For example, CSI should not be deployed to an environment where rotated samples part of input set  $Z$ .

Fig. 4 presents another fine-grained study which displays the relationship between normalized SOTA OOD prediction scores of an inlier sample  $X$  and  $T(X, \alpha)$  under some transformation  $\alpha$ . In alignment with previous benchmarks,  $\mathcal{F}(X)$  is usually close to zero. Predictions closer to zero indicate an inlier prediction. In most cases, we observe that for an  $X_1 \in X$ ,  $\mathcal{F}(X_1)$  is significantly lower than  $\mathcal{F}(T(X_1, \alpha))$ . In other words, the same OOD scoring function  $\mathcal{F}(Z)$  returns a significantly higher score on transformed samples. Samples with a score closer to one are more likely to be classified as OOD. Since both  $X_1$  and  $T(X_1, \alpha)$  are semantically in the inlier class, the gap between  $\mathcal{F}(X_1)$  and  $\mathcal{F}(T(X_1, \alpha))$  shows the error that the model will induce under transformation  $\alpha$ . An ideal OOD classifier that is robust to intra-class distribution shift will have a scatter plot where all points follow the diagonal red line, where for an  $X_2 \in X$ ,  $\mathcal{F}(X_2) == \mathcal{F}(T(X_2, \alpha))$ .

By now, the disparity in performance between SOTA OOD detection methods in existing benchmarks and our proposed benchmark is clear. For this reason, we emphasize the AUROC metric with existing benchmarks is not representative of real-world performance. We believe future research must consider our framework for meaningful advancements in OOD detection research.

#### 4.4. What is the effect of different layers on GS and OOD detection performance?

In Tab. 5, we obtain layers 1-4 from the convolutional base network and layer 5 from the layer before the final layer in the ResNet50. As data progresses deeper into the network, the model captures more semantic features. Initial layers capture limited semantics such as edges and curvatures. We observe that as the layers progress deeper, performance will increase but the generalizability score will decrease. This experiment was conducted using our evaluation framework over a subset of CIFAR-10, where 50 samples from each class were taken. The performance and GS are calculated under unrealistic (existing) setup and Augmentations (A) setup. Here we only used 90° rotation as augmentation.

Table 5. This table shows the effect of different layers of a pre-trained ResNet50 as an out-of-distribution (OOD) detection model in AUROC and GS in % on some samples in the CIFAR-10-R dataset under 90° rotation.

Layer	Mean	GS
Layer 1	46.78	-11.55
Layer 2	49.59	-4.71
Layer 3	51.58	-7.86
Layer 4	56.12	-5.04
Layer 5	61.03	-18.67

#### 4.5. Can We Train on Proposed Transformations to Improve OOD Detection Performance?

A naive solution to achieve high GS and AUROC on our proposed test datasets is to include all transformations  $\alpha$  into the training step. In reality, set  $\alpha$  can be of infinite size and it is impossible to completely cover all semantic-preserving distribution shifts during training. Even if we can form a subset of transformations in  $\alpha$ , the dataset creation and training will be computationally infeasible. In general, including such transformed samples during training does not solve the generalizability issue in OOD detection methods.

### 5. Conclusion

We have demonstrated the deficiency of existing OOD detection benchmarks because SOTA methods on such datasets are susceptible to distribution shifts even if the semantic meaning behind the image does not change. Such a deficiency is clearly indicative of the fact that SOTA methods cannot be deployed in the real world where distribution shifts are common. To prove that this is the case, we propose to create OOD testing datasets that contain semantically consistent distributionally shifted inlier samples. Such

samples are created through common corruptions and selected augmentations. To evaluate the efficacy of methods on such datasets, we introduce a generalizability score as a novel evaluation metric that easily measures how well a model should perform under a semantically-consistent distribution shift. We tested current SOTA OOD detection methods on these new benchmarks and observed that the higher the AUROC performance, the lower the generalizability score was. In particular, the method that had a bias against intra-class distribution shifts was the most heavily affected. Future research should stop solely focusing on AUROC on existing evaluation benchmarks because datasets in these benchmarks are not sufficient to reflect the wide variety of distribution shifts in the real world. We believe that OOD methods must consider and report this evaluation framework for a more realistic indicator of a method’s true performance. Strictly pushing for higher AUROC is a misguided goal, and future research that continues down this path may not be solving issues that are applicable to creating reliable and trustworthy machine learning models.

### References

- [1] Davide Abati, Angelo Porrello, Simone Calderara, and Rita Cucchiara. Latent space autoregression for novelty detection. In *Proceedings of the IEEE/CVF Conference on Computer Vision and Pattern Recognition*, pages 481–490, 2019. 3
- [2] Liron Bergman, Niv Cohen, and Yedid Hoshen. Deep nearest neighbor anomaly detection. *ArXiv*, abs/2002.10445, 2020. 3, 6
- [3] Liron Bergman and Yedid Hoshen. Classification-based anomaly detection for general data. *arXiv preprint arXiv:2005.02359*, 2020. 3
- [4] Paul Bergmann, Michael Fauser, David Sattlegger, and Carsten Steger. Mvtac ad – a comprehensive real-world dataset for unsupervised anomaly detection. In *Proceedings of the IEEE/CVF Conference on Computer Vision and Pattern Recognition (CVPR)*, June 2019. 6, 7
- [5] Yong Shean Chong and Yong Haur Tay. Abnormal event detection in videos using spatiotemporal autoencoder. In *International symposium on neural networks*, pages 189–196. Springer, 2017. 2
- [6] Yang Cong, Junsong Yuan, and Ji Liu. Sparse reconstruction cost for abnormal event detection. In *CVPR 2011*, pages 3449–3456. IEEE, 2011. 2
- [7] Jia Deng, Wei Dong, Richard Socher, Li-Jia Li, Kai Li, and Li Fei-Fei. Imagenet: A large-scale hierarchical image database. In *2009 IEEE conference on computer vision and pattern recognition*, pages 248–255. Ieee, 2009. 6
- [8] Dong Gong, Lingqiao Liu, Vuong Le, Budhaditya Saha, Moussa Reda Mansour, Svetha Venkatesh, and Anton van den Hengel. Memorizing normality to detect anomaly: Memory-augmented deep autoencoder for unsupervised anomaly detection. In *Proceedings of the IEEE/CVF Inter-*

*national Conference on Computer Vision*, pages 1705–1714, 2019. 2

[9] Ian J Goodfellow, Jean Pouget-Abadie, Mehdi Mirza, Bing Xu, David Warde-Farley, Sherjil Ozair, Aaron C Courville, and Yoshua Bengio. Generative adversarial nets. In *NIPS*, 2014. 2

[10] Dan Hendrycks and Thomas G. Dietterich. Benchmarking neural network robustness to common corruptions and perturbations. *ArXiv*, abs/1903.12261, 2019. 2, 4

[11] Dan Hendrycks, Mantas Mazeika, Saurav Kadavath, and Dawn Song. Using self-supervised learning can improve model robustness and uncertainty. *Advances in neural information processing systems*, 32, 2019. 3

[12] John Taylor Jewell, Vahid Reza Khazaie, and Yalda Mohsenzadeh. One-class learned encoder-decoder network with adversarial context masking for novelty detection. In *Proceedings of the IEEE/CVF Winter Conference on Applications of Computer Vision*, pages 3591–3601, 2022. 2

[13] Alex Krizhevsky, Geoffrey Hinton, et al. Learning multiple layers of features from tiny images. *Technical Report*, 2009. 5, 6, 7

[14] Shiyu Liang, Yixuan Li, and Rayadurgam Srikant. Enhancing the reliability of out-of-distribution image detection in neural networks. *arXiv: Learning*, 2018. 1

[15] Pramuditha Perera, Ramesh Nallapati, and Bing Xiang. Ocgan: One-class novelty detection using gans with constrained latent representations. In *Proceedings of the IEEE/CVF Conference on Computer Vision and Pattern Recognition*, pages 2898–2906, 2019. 2

[16] Tal Reiss, Niv Cohen, Liron Bergman, and Yedid Hoshen. Panda: Adapting pretrained features for anomaly detection and segmentation. *2021 IEEE/CVF Conference on Computer Vision and Pattern Recognition (CVPR)*, pages 2805–2813, 2021. 1

[17] Mohammad Sabokrou, Mahmood Fathy, and Mojtaba Hosseini. Video anomaly detection and localisation based on the sparsity and reconstruction error of auto-encoder. *Electronics Letters*, 52(13):1122–1124, 2016. 2

[18] Mohammad Sabokrou, Mohammad Khalooei, Mahmood Fathy, and Ehsan Adeli. Adversarially learned one-class classifier for novelty detection. In *Proceedings of the IEEE Conference on Computer Vision and Pattern Recognition*, pages 3379–3388, 2018. 2

[19] Mayu Sakurada and Takehisa Yairi. Anomaly detection using autoencoders with nonlinear dimensionality reduction. In *Proceedings of the MLSDA 2014 2nd Workshop on Machine Learning for Sensory Data Analysis*, pages 4–11, 2014. 2

[20] Mohammadreza Salehi, Hossein Mirzaei, Dan Hendrycks, Yixuan Li, Mohammad Hossein Rohban, and Mohammad Sabokrou. A unified survey on anomaly, novelty, open-set, and out-of-distribution detection: Solutions and future challenges. *arXiv preprint arXiv:2110.14051*, 2021. 1

[21] Vikash Sehwag, Mung Chiang, and Prateek Mittal. Ssd: A unified framework for self-supervised outlier detection. *arXiv preprint arXiv:2103.12051*, 2021. 3

[22] Jihoon Tack, Sangwoo Mo, Jongheon Jeong, and Jinwoo Shin. Csi: Novelty detection via contrastive learning on distributionally shifted instances. *ArXiv*, abs/2007.08176, 2020. 1, 2, 6

[23] Dan Xu, Elisa Ricci, Yan Yan, Jingkuan Song, and Nicu Sebe. Learning deep representations of appearance and motion for anomalous event detection. *arXiv preprint arXiv:1510.01553*, 2015. 2

[24] Jingkang Yang, Kaiyang Zhou, Yixuan Li, and Ziwei Liu. Generalized out-of-distribution detection: A survey. *arXiv preprint arXiv:2110.11334*, 2021. 1

[25] Muhammad Zaigham Zaheer, Jin-ha Lee, Marcella Astrid, and Seung-Ik Lee. Old is gold: Redefining the adversarially learned one-class classifier training paradigm. In *Proceedings of the IEEE/CVF Conference on Computer Vision and Pattern Recognition*, pages 14183–14193, 2020. 2

[26] M. Zaigham Zaheer, Arif Mahmood, M. Haris Khan, Mattia Segu, Fisher Yu, and Seung-Ik Lee. Generative cooperative learning for unsupervised video anomaly detection. In *Proceedings of the IEEE/CVF Conference on Computer Vision and Pattern Recognition (CVPR)*, pages 14744–14754, June 2022. 2

[27] Shuangfei Zhai, Yu Cheng, Weining Lu, and Zhongfei Zhang. Deep structured energy based models for anomaly detection. In *International Conference on Machine Learning*, pages 1100–1109. PMLR, 2016. 2

[28] Chong Zhou and Randy C Paffenroth. Anomaly detection with robust deep autoencoders. In *Proceedings of the 23rd ACM SIGKDD international conference on knowledge discovery and data mining*, pages 665–674, 2017. 2

[29] Bo Zong, Qi Song, Martin Renqiang Min, Wei Cheng, Cristian Lumezanu, Daeki Cho, and Haifeng Chen. Deep autoencoding gaussian mixture model for unsupervised anomaly detection. In *International Conference on Learning Representations*, 2018. 2